

ERROR REDUCTION FOR NUCLEAR BELT WEIGHERS

J.-G. OTTO

Department of Process Measurement and Control
University of Karlsruhe, FRG

Received June 14, 1988.

Abstract

Nuclear belt weighers have the advantage of contactless measuring bulk goods transported by conveyor belts while electromechanic belt weighers suffer from mechanical interferences. Up to now the profile error restricted the applicability of nuclear belt weighers to fine grained material.

In the paper the nuclear belt weigher and the profile error are analysed. A new scanning algorithm, implemented on a 8085-microprocessor system resolves the problem of profile error, improves precision and resolution in comparison to electromechanic belt weighers and generates an applicability of nuclear belt weighers in new fields.

Keywords: nuclear belt weigher, contactless measurement.

Introduction

In industrial processes which use or produce bulk goods, transport of those bulk goods is done by conveyor belts. For continuous processing it is necessary to determine and control the flow of mass at any time with belt weighers. *Fig. 1.* shows the principle of the conventional electromechanical dosage belt weigher.

The bulk goods are transported with the aid of the conveyor belt (2) from the storage bin (1) over several rollers until they are thrown off. One roller (3) is mounted on a weighing cell. The belt loading B is measured via the gravimetric force penetrating the weighing cell. A tachometer (4) gives the belt velocity v , which, multiplied by belt loading B , yields mass flow m . The difference between factual mass flow m and desired mass flow w feeds a controller (5), that controls the motor (6) and belt velocity, resp. to get the desired mass flow at the throw-off-point.

There are several disadvantages as to electromechanical belt weighers:

- expenditure for maintenance is high;
- calibration needs much time and additional weighing bins;

—the force on the weighing cell depends not only on the belt loading but on the tension of the conveyor belt, which varies with time, temperature and filling of the storage bin;

—mechanical interference factors and vibrations can make the output signal for mass flow very noisy;

—resolution of variations in belt loading is restricted by distance l_m of the neighbored conveyor rollers to the roller upon the weighing cell (l_m ranges from 0.5 meter up to 4 meters).

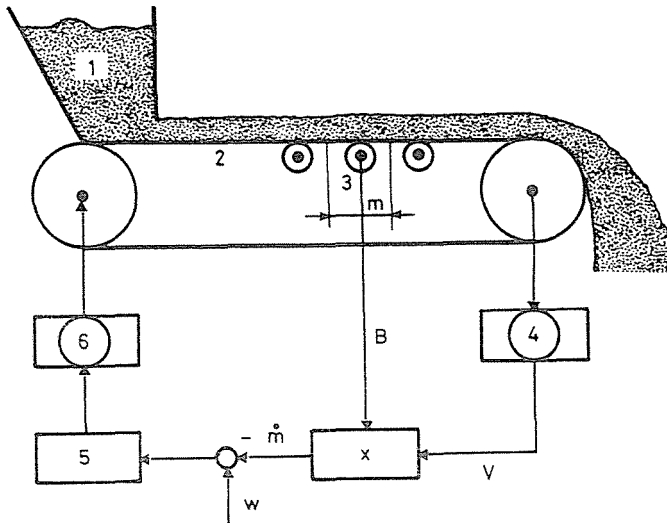


Fig. 1. Setup of an electromechanical dosage belt weigher. 1 storage bin 2 conveyor belt 3 electromechanical belt weigher 4 tachometer 5 controller 6 motor

The possibility to avoid the disadvantages of the electromechanical belt weigher is offered by the nuclear belt weigher as shown in Fig. 2. A rod source placed below the belt emits gamma radiation, which is attenuated by the belt loading. A cylindric scintillation counter above the belt detects the gamma radiation coming from the region of the conveyor belt. The amount of attenuation is a measure for the belt loading. The nuclear belt weigher has no moving parts, the measurement of the belt loading is contactless, so that no mechanical interference factors can disturb the output signal. However, nuclear belt weighers require that the kind of material on the belt is known and does not change, for the absorption of gamma radiation varies with atomic weight and moisture of bulk goods.

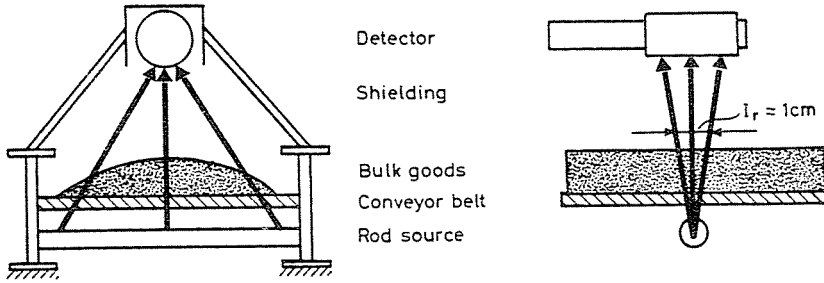


Fig. 2. Nuclear belt weigher

Basic physical properties

The law of absorption of gamma radiation according to Lambert-Beer reads in case of ideal gamma rays as:

$$Q_1 = Q_0 \exp\left\{-\int_0^{h_1} \rho(h)\mu(h)dh\right\}, \tag{1}$$

where the following notations are used:

- Q_0 quantum rate before entering material;
- Q_1 quantum rate after penetrating material;
- $\rho(h)$ density;
- $\mu(h)$ mass coefficient of absorption;
- h_1 thickness of the material layer.

In case of a constant ρ and μ , Eq. (1) reduces to

$$Q_1 = Q_0 e^{-\mu F}, \tag{2}$$

where

$$F = \int_0^{h_1} \rho(h)dh = \rho h_1 \tag{3}$$

denotes the mass per unit area.

The law of Lambert-Beer indicates, which amount of radiation reaches the detector without interaction of materia. The rest is involved into three major effects:

- *photoelectric effect*: a gamma quantum makes an electron leave the atom and vanishes.

- *pair production*: a gamma quantum decays within the Coulomb-field of the atom into an electron-positron pair.
- *Compton effect*: scattering of a gamma quantum by an atomic electron without destroying the gamma quantum.

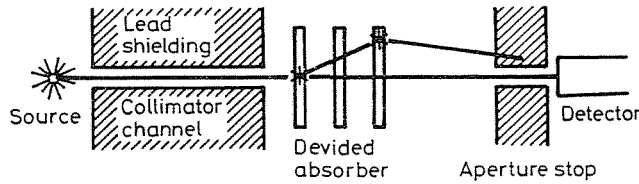


Fig. 3. An 'ideal' geometric setup

So the 'law of absorption' only denotes the number of gamma quanta reaching the detector, if the geometric setup is ideal as shown in Fig. 3., i.e. if a collimator selects one thin gamma ray, if the absorber is divided and if an aperture stop prevents the scattered radiation from reaching the detector. The real setup (see Fig. 2.) contains neither collimator nor aperture stop nor is the absorber divided. Therefore additional scattered radiation adds to the quantum rate according to Lambert-Beer and has to be considered by an additional build-up factor.

Determination of the build-up factor

Because the scattered radiation cannot be suppressed, the law of absorption has to be modified:

$$Q = Z(h) \cdot Q_0 e^{-\mu \rho h}. \quad (4)$$

We assume that the additional radiation Q_s reaching the detector is proportional to the part of radiation interacting with the bulk material:

$$Q_s \propto Q_0 - Q_1 = Q_0(1 - e^{-\mu \rho h}). \quad (5)$$

The total quantum rate reaching the detector is:

$$Q = Q_1 + Q_s = Q_1 + s(Q_0 - Q_1); s \geq 0. \quad (6)$$

A short calculation using the Taylor series of logarithm and exponential function yields:

$$-\frac{1}{h} \ln \frac{Q}{Q_0} = \mu\rho(1 - s) - \frac{s}{2} \mu^2 \rho^2 \cdot h \tag{7}$$

or

$$y = A_1 - A_2 \cdot h. \tag{8}$$

The constant terms A_1 and A_2 can be determined by linear regression; an example is given in *Fig. 4*.

The build-up factor follows by comparing equations (4) and (7):

$$Z(h) = e^{\mu\rho hs(1+\mu\rho h/2)} \tag{9}$$

The constants s and $\mu\rho$ are connected with A_1 and A_2 in the following sense:

$$(\mu\rho) = A_1 + \sqrt{\frac{A_1^2}{4} + 2A_2}, \tag{10}$$

$$s = \frac{(\mu\rho - A_1)}{\mu\rho}. \tag{11}$$

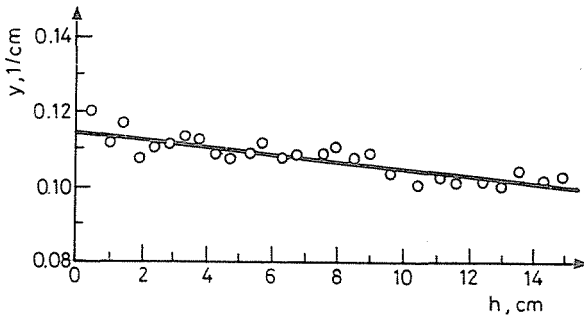


Fig. 4. Determination of the build-up factor in case of gravel ($\mu = 0.080 \text{ cm}^2/\text{g}$, $\rho = 1.51 \text{ g/cm}^3$) by linear regression, o measurements, - regression line

A_1 and A_2 are empirical constants containing information about the kind of material on the conveyor belt and about the geometric setup. To simplify the following considerations, we use A_1 and A_2 for calculating the quantum rate according to Lambert-Beer from the measured quantum rate and take the exponential law of absorption (*Eq. 1*) as the starting point of the considerations.

Conventional algorithm

The belt loading is defined according to Fig. 5. as

$$B = \frac{dm}{dx} = \int_{-b/2}^{b/2} \int_0^{h(y)} \rho(x, y, z) dz dy = b \cdot \bar{F} \tag{12}$$

where

$h(y)$ is the height of the material distribution

b is the width of the conveyor belt

and

$$\bar{F} = \frac{1}{b} \int_{-b/2}^{b/2} F(y) dy. \tag{13}$$

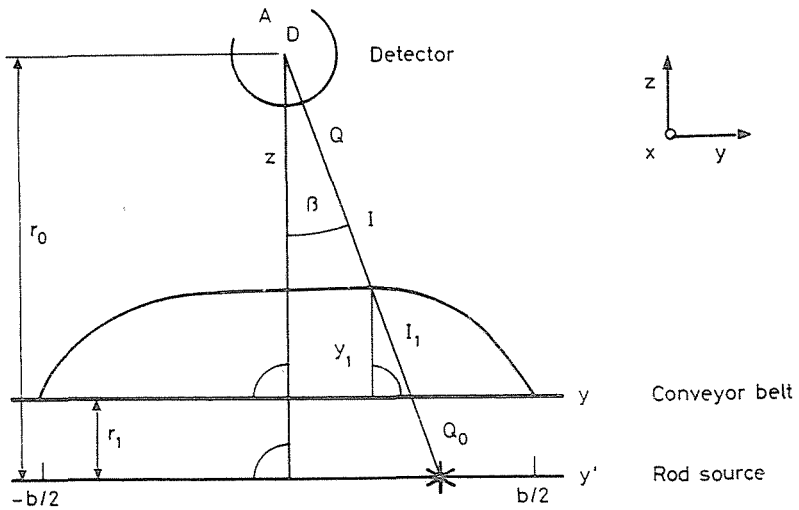


Fig. 5. Geometric setup and notations

\bar{F} is the mean mass per unit area and will be used equivalent to B . The conventional algorithm calculates the mean mass on the belt as a function of the total quantum rate Q reaching the detector, which is the integral of the quantum rate over the whole width of the conveyor belt:

$$Q = \int_{-b/2}^{b/2} Q_0(y) \exp(-\mu F(y)) dy, \tag{14}$$

where

$$Q_0(y) = Q'_0(y'(y)) \cdot A_D \cos \beta(y) \exp\{-\mu \delta F(y)\} / 4\pi r_0^2 \cdot f(y).$$

$Q'_0(y'(y))$ denotes the activity per unit length of the rod source, the second factor on the right side of Eq. (14) is a geometric factor, which considers size A_D of the detector, slope β of the gamma rays and the distance between source and detector. $f(y)$ indicates the attenuation caused by the housing of the rod source and the conveyor belt.

The total quantum rate is desired to be in a one-to-one correlation to belt loading B and/or mean mass per unit area \bar{F} . How can this be achieved? Let us consider the change of the total quantum rate ΔQ when changing a standard material distribution $F_N(y)$ by a small deviation $\Delta F(y)$ to $F(y)$.

$$F(y) = F_N(y) + \Delta F(y), \quad \Delta F(y) \ll F_N(y), \quad \mu \Delta F(y) \ll 1 \tag{15}$$

This leads together with Eq. (14) to

$$\Delta Q = -\mu \int_{-b/2}^{b/2} Q_0(y) \exp\{-\mu F_N(y)\} \Delta F(y) dy. \tag{16}$$

ΔQ should be a measure for changes in ΔB or $\Delta \bar{F}$:

$$\Delta Q \stackrel{!}{=} c_1 \Delta B = c_2. \tag{17}$$

Equation (17) is correct only in the case of a standard profile with

$$Q_0(y) = Q'_0(y) \exp\{-\mu F_N(y)\} = const. = Q_N. \tag{18}$$

So the rod source must be activated in a manner, that all gamma rays penetrating the standard material distribution contribute the same amount to the total quantum rate. Then the total quantum rate indeed leads to the mean mass, $\Delta \hat{F}$, per unit area via the conventional algorithm (reversal of the exponential law of absorption):

$$\hat{\Delta F} = -\frac{1}{\mu} \ln \frac{Q}{Q_0}. \quad (19)$$

$\hat{\Delta F}$ is a good estimation for $\overline{\Delta F}$, if the deviation $\Delta F(y)$ from the normal profile $F_N(y)$ is small. In case of a fine-grained materials this condition can be met approximately by slipping the material. In case of a coarse-grained material the method does not work.

The profile error

For large deviations from the normal profile the conventional algorithm is not correct, there is an error, the so-called profile error, which, up to now, restricts the use of nuclear belt weighers. Let us assume a large but constant deviation $\Delta F(y) = \text{const} = \overline{\Delta F}$. The conventional nuclear belt weigher estimates

$$\hat{\Delta F} = -\frac{1}{\mu} \ln \frac{Q_N \int_{-b/2}^{b/2} \exp\{-\mu \Delta F(y)\} dy}{Q_N b} = \overline{\Delta F}. \quad (20)$$

Constant deviations from the standard profile cause no profile error. Therefore it is sufficient to consider only material distributions with

$$\int_{-b/2}^{b/2} \Delta F(y) dy = 0. \quad (21)$$

In case *Eq.* (21) is not fulfilled, the profile can easily be transformed by adding a constant term to that case without changing the profile error.

Fig. 6. shows a standard profile F constant over the whole breadth of the belt and two deviations, which represent slowly variable (*a*) and discontinuous profiles (*b*).

$$\frac{\Delta F(y)}{F} = \frac{2c}{b} y; \quad (22a)$$

$$\frac{\Delta F(y)}{F} = \pm c. \quad (22b)$$

Parameter c denotes the maximum deviation from the standard profile. Both profiles have $\overline{\Delta F} = 0$. The relative profile errors follow from *Eq.* (19) and from the condition for maximum sensitivity ($\mu = 1/F$):

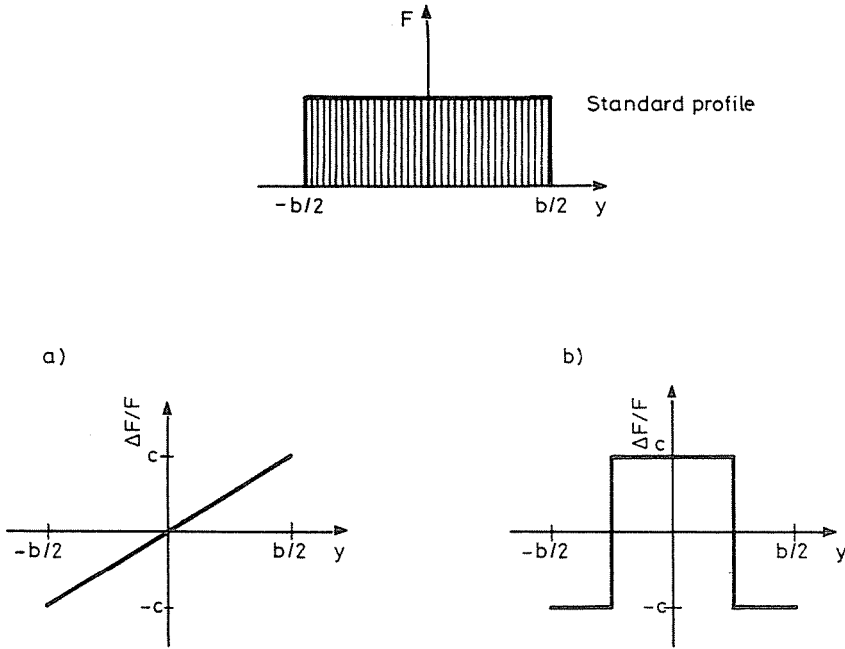


Fig. 6. Standard profile and deviations

$$\frac{\hat{\Delta F}}{F} = -\ln\left(\frac{1}{c} \sin hc\right) \tag{23a}$$

$$\frac{\hat{\Delta F}}{F} = -\ln(\cos hc) \tag{23b}$$

In case a) the maximum value of $c = 1$ means that the fourth part of the belt loading is shifted from the left to the right half of the belt, resulting in a profile error of -16% , in case b) $c = 1$ describes a situation when the material is concentrated on half of the belt, width resulting in an error of -43% (see also Fig. 7.).

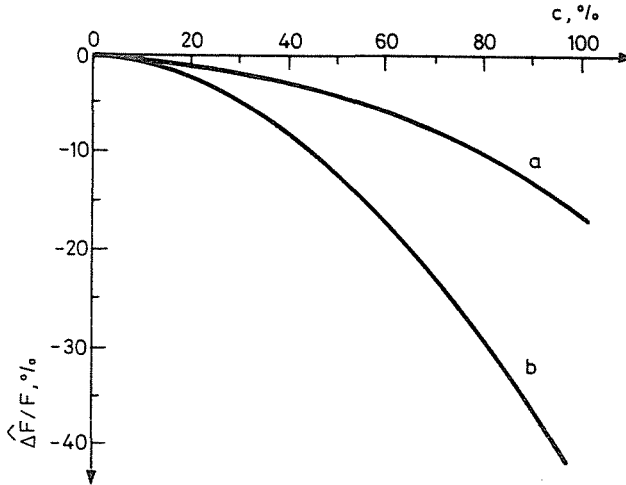


Fig. 7. Profile error of the profiles in Fig. 6 in dependence of maximum deviation c

The scanning method

The profile error exists, because the total quantum rate Q and belt loading \bar{F} are not correlated one-to-one, if the profile form is arbitrary. The only way to resolve the profile error is to analyse each gamma ray separately instead of the total quantum rate. For the purpose different setups are possible (see GLÄSER and BEER, 1979; OTTO, 1986). We found a way to modify a conventional commercial nuclear belt weigher (see Fig. 8.), which has been built by the laboratory of Prof.-Dr. BERTHOLD (1979).

Between the rod source (consisting of a chain of 16 point sources Cs^{137} , 1 mC activity each) and the belt a lead cylinder is placed with N pairs of slots helically arranged on a screw line. Driven by a motor, the cylinder opens the way of the gamma rays from rod source to detector part by part, the material profile is scanned with N scanning intervals. The partial quantum rate measured within the scanning intervals is used to evaluate the loading of the intervals, separately. The scanning algorithm computes the mean value of the loadings $\hat{\Delta F}_i$ of the N intervals.

$$\Delta \hat{F}_s = \frac{1}{N} \sum_{i=1}^N \Delta \hat{F}_i = \frac{1}{N} \sum_{i=1}^N -\frac{1}{\mu} \cos \beta_i \ln \left(\frac{Q_i}{Q_{Ni}} \right). \quad (24)$$

This calculation as well as the control of the measuring system is done by a 8085 microprocessor system.

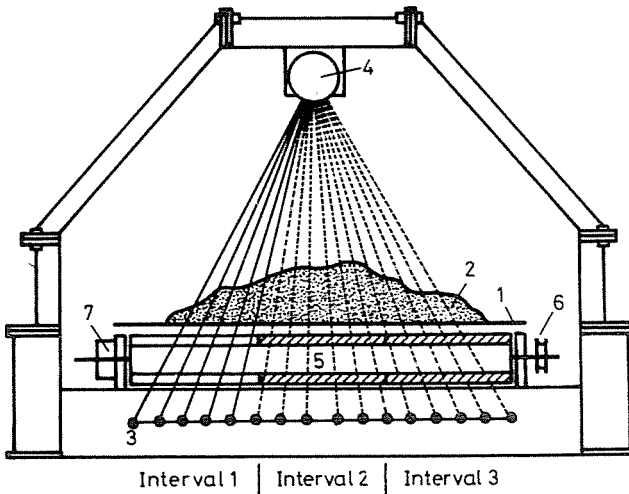


Fig. 8. Nuclear scanning belt weigher; 1 conveyor belt, 2 bulk goods, 3 point sources (16, 1 mC activity each), 4 scintillation counter, 5 lead cylinder with slots, 6 pulley drive, 7 revolution counter

If there is an adequately high number of scanning intervals ($N \rightarrow \infty$), the profile variations within the intervals can be neglected and the profile error disappears. In practice N is limited. The ratio of the error of the scanning method to the error of the conventional nuclear belt weigher is in case of the characteristic profiles of the previous chapter:

$$\frac{\Delta \hat{F}_s}{\Delta \hat{F}} = \frac{1}{N^2} \quad \text{for profile } a; \tag{25a}$$

$$\frac{\Delta \hat{F}_s}{\Delta \hat{F}} = \frac{N_1}{N} \quad \text{for profile } b \tag{25b}$$

where N_1 is the number of discontinuities.

A numerical simulation of the profile error in dependence of maximum deviation c and the number of scanning intervals is shown in Fig. 9. A constant material distribution ($F_N(y) = const.$) is superponed with a sinusoidal deviation (1.2 periods). To get a desired error less than a given limit, for example 2%, for a maximum deviation of $c = 60\%$ at least $N = 4$ scanning intervals are necessary.

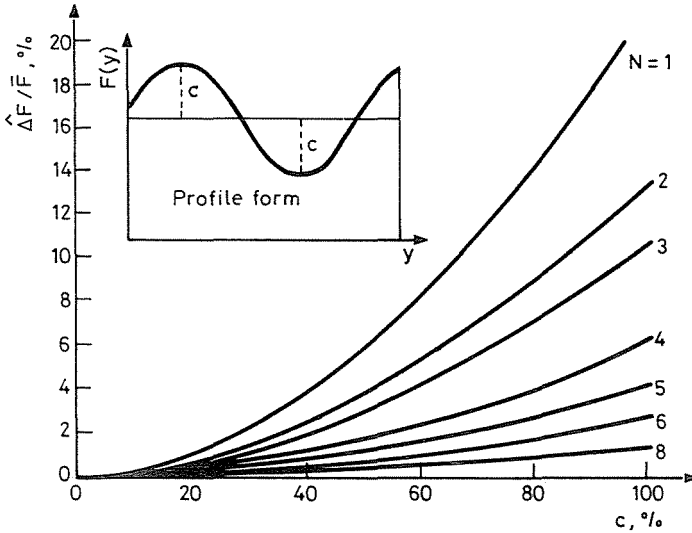


Fig. 9. Profile error of a sinusoidal disturbed profile form (1.2 periods) in dependence of maximum deviation c

Bias due to quantum stochastics

Emission and absorption of gamma quanta are more or less but stochastic processes. So the law of decay as well as the law of absorption are statistical ones which are exactly correct only in the mean. The number M of detected gamma quanta within measuring time T will fluctuate even if the belt load remains constant. The fluctuations are described by Poisson's distribution $p(M)$:

$$p(M) = \frac{1}{M!} e^{-QT} (QT)^m. \tag{26}$$

Q is the expectation value of the quantum rate according to Lambert and Beer, the mean value of quanta per measuring time is $\bar{M} = Q \cdot T$. The variance of detected quanta is according to Poisson's distribution

$$\sigma_M^2 = \bar{M} = QT. \tag{27}$$

Because of the non-linearity of the Lambert-Beers law the fluctuations lead to a bias, whose expected value is:

$$\mathcal{E}\{\hat{F} - \bar{F}\} = \frac{\mathcal{E}\{M^2 - \bar{M}^2\}}{2\mu\bar{M}_A^2} = \frac{\sigma_M^2}{2\mu\bar{M}_A^2} \tag{28}$$

The expected value of the relative bias using Eq. (27) is:

$$\mathcal{E}\left\{\frac{\hat{F} - \bar{F}}{\bar{F}}\right\} = \frac{Q}{2\mu\bar{F}TQ_A^2} \approx \frac{1}{2Q_A T} \tag{29}$$

The scanning algorithm (24) has to be corrected by (29).

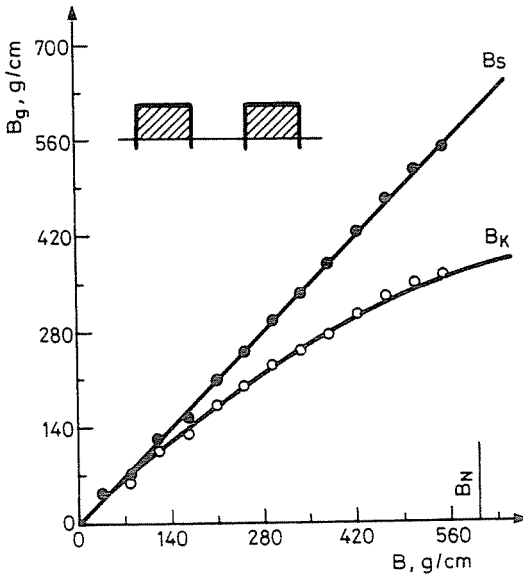


Fig. 10. Measurement with gravel, three-step profile
B_g measured belt loading, *B* true belt loading
 o conventional algorithm
 • scanning algorithm
B_N belt loading of the normal profile

Experimental results

Static measurements, i.e. not time varying profiles, were made concerning many material distributions. One set of measurements can be seen in

Fig. 10., the profile form has always a gap in the middle third. The graph shows measured belt loading versus real belt loading. Scanning with $N=3$ intervals gives the right values (B_s), while the conventional method suffers from large profile errors (B_k). The continuous lines represent the values expected by the theoretical considerations. The experimental results confirm the theory of the profile error.

A dynamic measurement with time varying profile forms is shown in Fig. 11. The output signal of the electromechanical belt weigher (a) is rather noisy. The signal of the nuclear belt weigher (b,c) is smooth during constant profiles. The profile error appears in the deviation of curve (c) from the right value of curve (b) in profile 1.

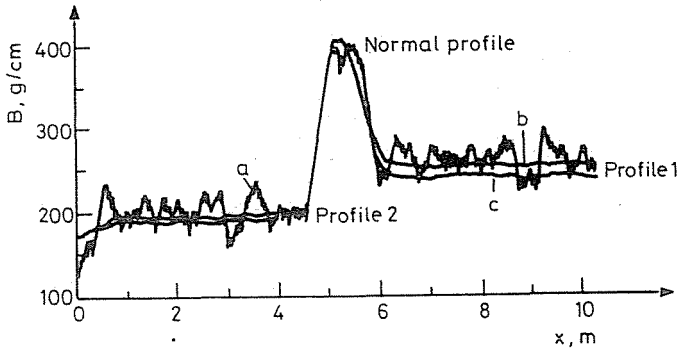


Fig. 11. Comparison of an electromechanical belt weigher (a), a nuclear belt weigher modified by scanning algorithm (b) and a conventional nuclear belt weigher (c)

The signal of the nuclear belt weigher was lowpass filtered to get the same resolution. Because of $l_r \ll l_m$ the resolution of the original signal is much better than that of the electromagnetic belt weigher (Fig. 12.).

Conclusion

The nuclear belt weigher modified by the scanning method yields a much smaller profile error than the conventional nuclear belt weigher and a higher resolution than the electromechanical belt weigher. The measurement of belt loading works contactless, thus defeating noise coming from mechanical interferences. The nuclear belt weigher can now be used also in case of coarse grained materials and rapidly varying profiles.

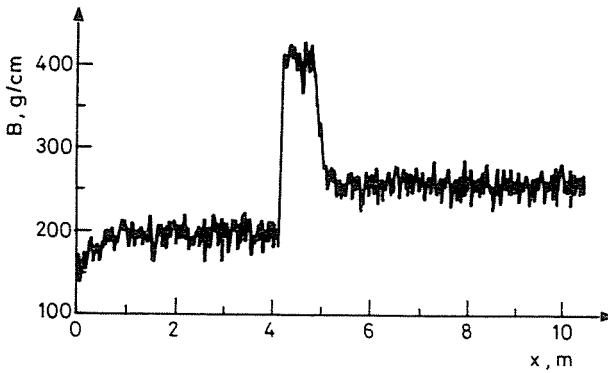


Fig. 12. Output signal of nuclear scanning belt weigher without lowpass filtering

References

- GLÄSER, M. – BEER, M. (1979): Radiometrische Streckenbelegungssonden (Radiometric load sensors). *Agrartechnik*, Vol. 29, No. 7 pp. 305–7. (In German)
- OTTO, J. (1986): Profilunabhängige radiometrische Messung bei Bandwaagen (Profile independent radiometric measurements in belt weighers). *VDI-Fortschritt Bericht*, Ser. 8, No. 111. Düsseldorf, VDI. (In German)
- Laboratorium Prof. Dr. BERTHOLD (1979): Bandwaage LB387. Wildbad, FRG. (In German)

Address:

Dr. Johannegeorg OTTO
 Institut für Prozessmesstechnik und Prozessleittechnik
 Universität Karlsruhe
 Hertzstr. 16, D-7500 Karlsruhe 21, FRG